Open Access
J. Glob. Innov. Agric. Sci., 2024, 12(2):315-325
ISSN (Online): 2788-4546; ISSN (Print):2788-4538
DOI: https://doi.org/10.22194/JGIAS/24.1182
http://www.jgiass.com

Prediction of Aflatoxin Contamination in Cocoa Beans Using UV-Fluorescence Imaging and Artificial Neural Networks for Enhanced Detection

Muhammad Syukri Sadimantara[1,2*], Bambang Dwi Argo[3], Sucipto Sucipto[1], Dimas Firmanda Al Riza[3] and Yusuf Hendrawan[3]

[1]Department of Agroindustrial Technology, Universitas Brawijaya, Malang, 65145, Indonesia;[2] Department of Food Science and Technology, Universitas Halu Oleo, Kendari, 93231, Indonesia; [3]Department of Biosystems Engineering, Universitas Brawijaya, Malang, 65145, Indonesia
*Corresponding author's e-mail: syukrisadimantara@uho.ac.id

This study introduces an innovative approach to predicting aflatoxin contamination levels in cocoa beans by leveraging an optimized Artificial Neural Network (ANN) model coupled with UV-fluorescence imaging. *Aspergillus flavus*-inoculated cocoa beans underwent a 7-day incubation period, and UV lamp-based image acquisition facilitated data collection. Leveraging 289 color-texture features, the developed ANN model exhibited highly promising predictive capabilities. Validation results indicate a remarkably low Mean Square Error (MSE) of 0.0087 and a high R-value of 0.9910, affirming the efficacy of the proposed model. The seamless integration of UV-fluorescence imaging and ANN presents a viable and accurate alternative for detecting aflatoxin in cocoa beans, thereby enhancing food safety practices within the cocoa industry.
Keyword: Aflatoxin Contamination, Artificial Neural Network, Cocoa Beans, Food Safety, UV-Fluorescence Imaging, Machine Learning.

INTRODUCTION

The contamination of agricultural products with aflatoxin has become a pressing global concern, given that an estimated 4.5 billion individuals are susceptible to its adverse effects (Shabeer *et al*., 2022). Aflatoxin is a secondary metabolite produced by *Aspergillus flavus*, which has been found to have carcinogenic effects (Kong *et al*., 2022), *hepatotoxicity* and *teratogenicity* (Van Der Fels-Klerx *et al*., 2016), as well as affecting fetal health (da Silva *et al*., 2021). It commonly affects agricultural products, particularly grains and cereals such as corn (Cabrera-Meraz *et al*., 2021), peanuts (Osaili *et al*., 2023), rice (Dachoupakan *et al*., 2013), and cocoa beans (Oliveira *et al*., 2009). Cocoa beans are a widely traded commodity, internationally renowned for their high export value and use as a primary ingredient or additive in various food products (Wahyuni *et al*., 2016). The total volume and its derivatives traded in 2018-2019 amounted to $50.9 billion, with a 2.12% surge in the export value of the products (Vivek *et al*., 2019). However, cocoa beans are susceptible to aflatoxin contamination in the supply chain, owing to unfavorable storage and production conditions (Copetti *et al*., 2014). These conditions provide a conducive environment for *Aspergillus flavus* and *Aspergillus parasiticus*, which serve as sources of aflatoxin, to thrive. Early detection of the contamination is necessary due to several reasons such as market awareness of product quality (Ketney, 2015), and strict regulations governing the maximum intake of aflatoxin by international institutions such as the European Commission set at 20 ppb (European Commission, 2014). The thermostable characteristics of aflatoxin render it a formidable challenge to eradicate (Adriansyah *et al*., 2022). Currently, Computer vision has emerged as a viable alternative to traditional chemical methods, such as Liquid Chromatography-Mass Spectrometry (LCMS), for detecting aflatoxin contamination in various agricultural products (Fang *et al*., 2022). This approach can accurately quantify mycotoxin contamination, but has drawbacks such as being destructive, relatively expensive, time-consuming, and requiring expertise from laboratory technicians (Hassoun and Karoui, 2015). Computer vision approaches in mycotoxin detection include Color Imaging (Polisenska, 2011), Near-infrared (NIR) Spectroscopy (Mallmann *et al*., 2020), Mid-infrared (MIR) Spectroscopy (Kaya-celiker *et al*., 2015), Near-infrared (NIR) Hyperspectral Imaging (Thiruppathi, 2016), and X-Ray Imaging (Du *et al*., 2019). Every

Sadimantara, M.S., B.D. Argo, S. Sucipto, D.F. Al Riza and Y. Hendrawan. 2024. Prediction of Aflatoxin Contamination in Cocoa Beans Using UV-Fluorescence Imaging and Artificial Neural Networks for Enhanced Detection. Journal of Global Innovations in Agricultural Sciences 12:315-325.
[Received 13Nov 2023; Accepted 13 Dec 2023; Published 30 May 2024]

technology possesses its unique set of advantages and disadvantages. For instance, the "Color Image" technology boasts a detection accuracy as high as 89%. However, it is restricted by a limited electromagnetic range, rendering it incapable of detecting mycotoxin contamination in its early stages (Tallada *et al*., 2011). Ultraviolet (UV)-Induced-fluorescence Imaging can be an alternative for detecting aflatoxin by using the excitation-emission properties of fluorescent light, where every organic material including aflatoxin has different properties (Cozzini *et al*., 2008). In addition, aflatoxin has an excitation and emission wavelength of 365 nm and 455 nm (Kamilaris and Prenafeta-Boldú, 2018). Study on the utilization of fluorescence properties has been conducted, such as *Hyperspectral Fluorescence imaging* for detecting aflatoxin in corn (Hruska *et al*., 2017). The hyperspectral approach entails a relatively high cost for the acquisition of specialized equipment. Therefore, an alternative approach that is simpler and more cost-effective may be deemed necessary. Rotich et al. (2020) used a 365 nm LED as an excitation light source and a color camera to record the optical characteristics of UV-induced fluorescence images in the visible spectrum. By exciting the target fluorophore at a specific wavelength, it emits light in the visible region, which enables the use of simplified imaging techniques. However, fluorescence imaging has its limitations as dust in the air and oil in grains fluoresce in the ultraviolet range. This can lead to reduced accuracy in the detection of aflatoxin with only blue-green fluorescence under UV light (Gao *et al*., 2021). Therefore, additional image analysis may be necessary to overcome this challenge.

One of the factors that affect the accuracy of predicting levels of aflatoxin contamination is the selection of an Artificial Intelligent (AI) approach. There are several approaches in machine vision, such as ANN Feed Forward (Anami *et al*., 2015) ANN multi-layer perception (Bhensjaliya and Vasava, 2019), Support Vector Machine (Kaur and Singh, 2013), K-nearest neighbor (Patil *et al*., 2011), and Bayesian classifier (Venora *et al*., 2009) with different classification accuracy. ANN is a machine learning technique that has shown promising results in terms of accuracy, as reported in various studies. For instance, Hendrawan *et al*. (2019) used ANN to predict the phenol, pH, and purity of civet coffee, while Chen *et al*. (2023) employed it to estimating the water content, water-soluble protein and total sugar in royal jelly. The success of these studies showcases the potential of ANN in various fields, including food science and technology. In both studies, low validation MSE and high correlation values were obtained using ANN backpropagation.

Based on the above explanation, this study predicts aflatoxin contamination levels in cocoa beans, namely aflatoxin-free cocoa beans, those contaminated below and above the threshold limit based on LC-MS quantification, UV-induced fluorescence imaging acquisition system, followed by predicting the level of contamination through ANN backpropagation. This study aimed to provide an alternative for predicting aflatoxin in cocoa beans by using the fluorescence properties to provide a higher level of accuracy than other approaches.

MATERIALS AND METHOD

***Materials*:** The materials used included Pure strain A. flavus (Inacc F44) was collected from Lembaga Ilmu Pengetahuan Indonesia (LIPI) microbiology laboratory, Cibinong, Indonesia. Forastero cocoa beans that had been fermented for 5 days with a shelf life of 3 months in a warehouse from the Pusat Penelitian Kopi dan Kakao, Jember, Indonesia. The fermented beans were unbroken, free of mycotoxin contamination and had a low moisture content of 6%. The chemicals used were aqua dest, NaCl, methanol, alcohol, and potato dextrose broth (PDB) media.

The hardware used was image acquisition mini research consisting of a Canon EOS 700D DSLR camera with dimensions of 133 × 100 × 79 mm, equipped with a PL filter. The camera had 18MP resolution specifications with a CMOS sensor, ISO 100-12800, a shutter speed of 30-1/4000 seconds, and Full HD video. 22.3 x 14.9 mm CMOS sensor size. UV Lamp Model: LDR2-100UV3-365-N, input 24V(DC)/23W, manufactured by CCS Inc. The power supply had 30V/5A Specification with code MDB-K305D. A LED Pulse Controller, Brand GARDASOFT with model PP820C, which was equipped with 8 channels that can regulate a maximum current of 20A was used, with an input of 12-48V. A mini studio frame was assembled from several angles with a thickness of 2 mm combined using 10mm nuts and a Lenovo laptop with Intel Core i5-7200u specifications, 2.50GHz CPU 2.71GHz, and 16GB memory. The software used was a feature extraction program based on Visual Basic 6.0 for color and texture feature extraction. Aflatoxin quantification using Liquid Chromatography Mass Spectrometry (LCMS)/MS brand (Hitachi L 6200).

***Fungus inoculum*:** Pure *A. flavus* was cultured in 10 mL of nutrient broth to obtain fungal inoculum, which was then incubated at room temperature for 3 days. The culture was resuspended and re-inoculated in 100 mL of NB media and incubated for 3 more days at room temperature. Subsequently, the resulting culture was inoculated in 1000 mL of NB media and incubated for 3 more days at room temperature to obtain a stock inoculum for cocoa beans inoculation. The fungal inoculum was added at a rate of 60 mL/kg of cocoa beans and incubated at 30°C and 90% RH until day 7 after inoculation with *A. flavus*.

***Measurement of aflatoxin levels*:** The samples' levels of aflatoxin were assessed using LCMS. The LC system contained a Shimadzu pump type LC-10AD (Shimadzu, Kyoto, Japan), an Agilent 1100MSD SL mass spectrometry detector with an orthogonal ESI nozzle, a fluorescence detector (RF-10AXL) from Shimadzu, an auto-injector from

Shimadzu (SIL-10A), and a control system from Shimadzu (SCL-10A). The AF standard and pure samples were dissolved in 1 ml of mobile phase solution, and 6 µL of the solution was added to the LCMS/ESI. Protonated molecules, [M+H]+, with a residence duration of 1,000 ms per ion, were detected in all of the tested AFs. AFB_1, AFB_2, AFG_1, and AFG_2 were the targets of selected ions (m/z) measured at 313, 315, 329, and 331, respectively For LC analysis, 0.1 mL of TFA was added to the test tube holding the pure sample or the aflatoxin working standard. The tube was vortexed, then diluted with 0.9 ml of a 1:9 acetonitrile-water solution, and left to stand at room temperature for 15 minutes without light. The resultant solution was then examined using 20 µL of reverse phase LC analysis. Aflatoxin was found using Electrospray ionization in Multiple reaction monitoring modes. The total number of chemicals contained in each sample was estimated using the results of the LC/MS-MS data analysis by providing the chromatogram in the form of peaks and the molecular weight of the compounds contained in the extract. Each measurement was performed three times.

***Image acquisition and feature extraction*:** The image acquisition of cocoa beans was conducted for up to seven days after *A. flavus* inoculation, using a Canon L300 camera. The generated photographs were saved as JPG files with a 400 x 600 pixel resolution. The Picture was taken in a studio equipped with a ring-type UV LED lamp with a 365 nm wavelength, manufactured by CCS Inc., Japan. The UV lamp was placed 350 mm from the sample unit, and the average radiation on the sample plane was 6.9 Wm^2. Furthermore, a UV bandpass filter was used to filter out the reflected light by placing a filter between the UV light source and the camera. It performs similarly to a UV cut filter but only lets 0.3% of 365 nm to pass through. The EOS Kiss 7 (Canon Inc., Japan) with ISO 200, F-5.6, and manual exposure of 1/3 second was utilized in the image acquisition component to record fluorescence images. This camera was set 450 mm from the sample location. The image capture device is attached to the light source by an optic wire and measures 18.5 cm × 18.5 cm × 29 cm., as shown in Figure 1.

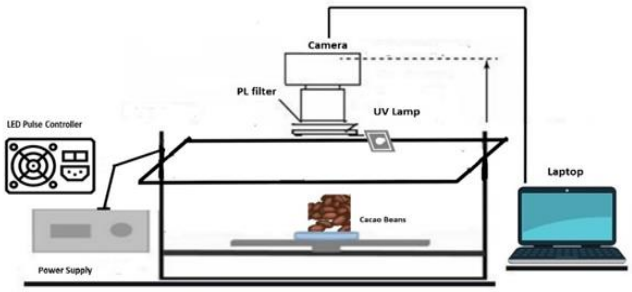

Figure. 1. Image acquisition unit.

The number of fluorescence images was 300, with each consisting of 12 cocoa beans. The obtained images were grouped according to the LCMS test results into 3 categories, namely no aflatoxin, and contamination below and above the limit of quantification. Subsequently, the color-texture features of the contaminated cocoa beans images were extracted using a Visual Basic-based program. The program was capable of breaking down the color channels into L*a*b, LUV, LCH, XYZ, gray, CMYK, and CMY (Ford and Alanrobertsrdbbccouk, 1998), as well as Hue-Saturation-Lightness (HSL) and Hue-Saturation-Value (HSV) (Saravanan *et al*., 2016) to obtain 26 color indices ; red, green, blue, gray, hue (HSL dan HSV) Saturation(HSL), lightness(HSL), Saturation (HSV), Value(HSV), X, Y, Z, CMY(C), CMY(Y), CMYK(M), CMYK(Y), CMYK(K), L (L*a*b;LCH;LUV), a (L*a*b) dan b (L*a*b), LCH (C), LCH (H), LCH (U), dan LUV(V). The color index had 10 texture features: energy, contrast, correlation, variance, different inverse moment, entropy, homogeneity, sum mean, cluster tendency, and maximum probability (Hendrawan *et al*., 2019) analyzed using the Harralick equation for texture feature extraction (Haralick *et al*., 1973). There were 26 color indices for 10 textures, resulting in 260 features. This study also used Excess Red Index (ERN) (Marcial-Pablo *et al*., 2019), Excess blue index (EBN), and Excess green index (EGN) (Zhang *et al*., 2021) resulting in a total of 289 color-textural features.

***ANN modelling*:** The ANN modeling started with selection using the *Waikato Environment for Knowledge Analysis* (WEKA) 3.8.6 software to obtain relevant features, while the optimization of ANN performance was conducted using Matlab R2021a software. The image was divided into 80% (240 images) and 20% (60 images) for training and validation data. Furthermore, the algorithm used was backpropagation because of its ease of programming and ability to manipulate large amounts of data (Amin *et al*., 2019). Normalization of input and output data was required before proceeding to the next step. The input layer consisted of color-texture features, while the output layer included the level of aflatoxin contamination. In addition, sensitivity analysis was performed to obtain ANN structure for the best MSE and R. This was performed by trial and error of various activation functions (tansig, logsig, and purelin), learning functions, momentum, and learning rate (0.5, 0.9), hidden layer (1, 2), and number of nodes in the hidden layer (10, 20, 30) with the lowest validation MSE parameter.

RESULTS

***Quantification of aflatoxin levels in Aspergillus flavus inoculated cocoa beans*:** Based on the LCMS test results, AFB_1, AFB_2, AFG_1, and AFG_2 retention times were 5.71, 4.54, 5.3, and 5.14 minutes, respectively. The concentrations of AFB_1, AFB_2, AFG_1, AFG_2, and total AFs in cocoa bean samples on day 7 gave the response of peak formation at the same time as the aflatoxin standard in B_1 and G_1 types. However, there was a different retention time from the

aflatoxin standard for B_2 and G_2, indicating that AFB_1 and AFG_1 were present in cocoa beans. the chromatogram of aflatoxin on the sample on day 7 was 97.8 ppb total aflatoxin, which was included in the category of exceeding the threshold of 15 ppb as shown in Figures 2 and 3:

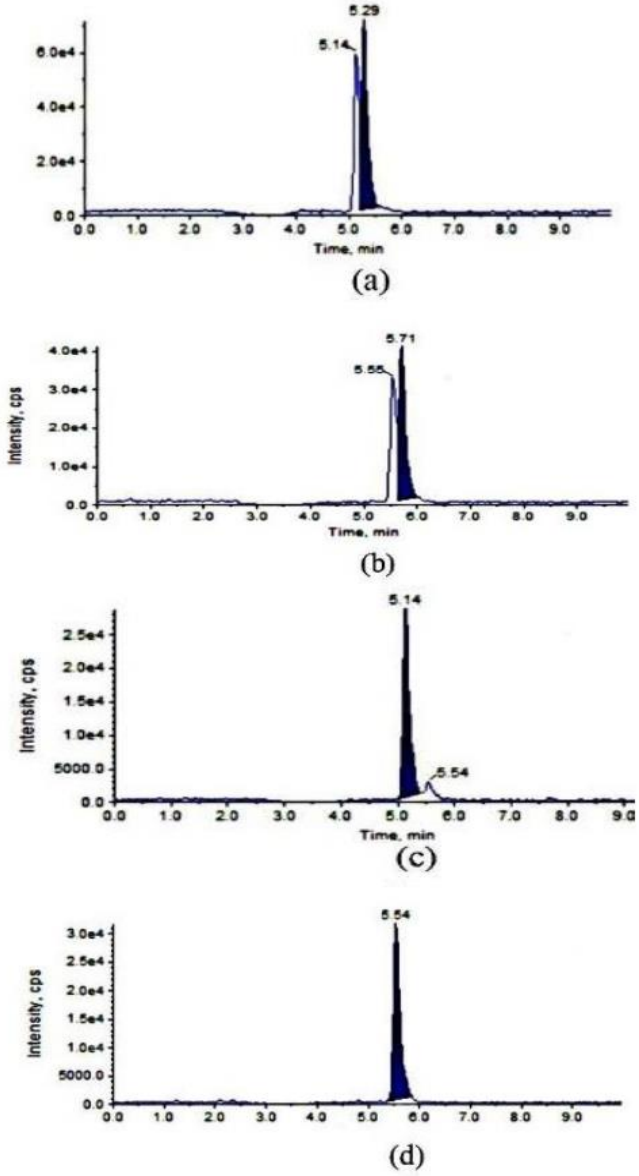

Figure 2. Standard chromatogram of AF. (a) AFG_1 standard chromatogram. (b) AFB_1 standard chromatogram, (c) AFG_2 standard chromatogram, (d) AFB_2 standard chromatogram

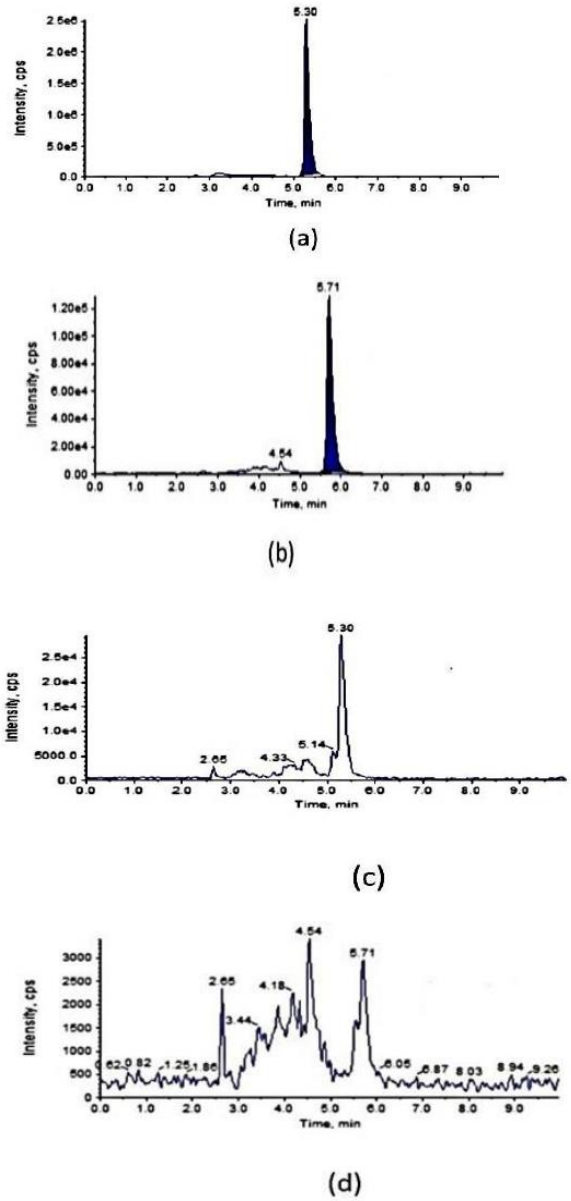

Figure 3. Sample chromatogram. (a) AFG_1 sample chromatogram (b) AFB_1 sample chromatogram (c) AFG_2 sample chromatogram (d) AFB_2 sample chromatogram

Quantification of aflatoxin levels in Aspergillus flavus inoculated cocoa beans presented in Figure 4.

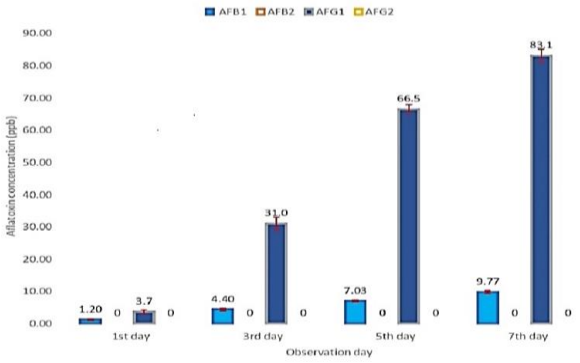

Figure 4. Changes in aflatoxin levels after inoculation of *A. flavus* on cocoa beans

In Fig. 4, the increase in AFB_1 and AFG_1 levels occurred in the *A. flavus* inoculation treatment. AFG_1 had the highest increase in aflatoxin levels, which was 83.10 ppb on day 7, followed by AFB_1 at 9.77 ppb. Meanwhile, aflatoxin levels of contamination were significantly different in each observation. The reporting limit, which indicates the minimum limit for aflatoxin levels that can be detected by LCMS = 1 ppb, showed no detection in the control treatment, as well as AFB_2 and AFG_2, were not detected in the AF inoculation treatment from day 1 to 7.

Image acquisition and analysis: The fluorescence image of cocoa beans obtained is shown in Figure 5.

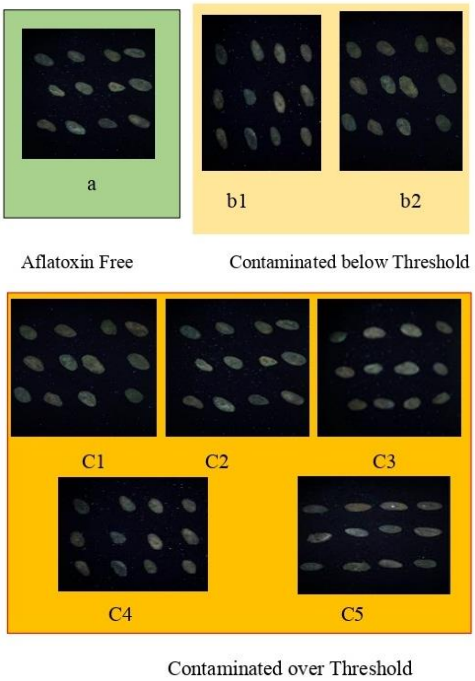

Figure 5. Fluorescence image of cocoa beans from *A. flavus* inoculation on days 1-7.
a) control, (b1) 1st day, (b2) 2nd day, (C1) 3rd day, (c2) 4th day, (c3), 5th day, (c4) 6thday, (c5) 7th day

In Fig. 5, cocoa beans image can be observed with blue UV light emission on day 7. This emission occurs when fluorophores are excited by UV light at a specific wavelength, resulting in a longer wavelength. AFB_1 and AFB_2 have blue fluorescent colors, while AFG_1 and AFG_2 have green colors (Galaverna and Dall'Asta, 2012).

***Prediction of the level of aflatoxin contamination in fluorescent images using ANN*:** Feature selection uses 3 attribute evaluators, namely OneR attribute, reliefF, and gain ratio. The result yields a ranking of the top 10 attributes, consequently enhancing input efficiency for ANN as presented in Table 1.

Table 1. Feature selection of aflatoxin-contaminated cocoa beans in fluorescence images.

Attribute Evaluator	Method	Image Features	Weight	Rank
OneRattribute	Ranker	CMY_Y Mean	88.333	1
		CMYK_M Entropy	74.667	2
		CMYK_M Correlation	74.000	3
		CMYK_M Energy	73.667	4
		CMYK_M Contrast	73.667	5
		CMYK_M Inverse	73.667	6
		CMYK_M Homogeneity	73.333	7
		Hue Contrast	73.333	8
		S_hsv Inverse	73.000	9
		CMYK_M Max.Prob.	73.000	10
ReliefF	Ranker	CMY_Y Mean	0.6176	1
		S_hsl Homogeneity	0.4470	2
		CMYK_M Cluster	0.4255	3
		CMYK_M Variance	0.4253	4
		LCH_C Variance	0.4004	5
		Hue Homogeneity	0.3987	6
		LCH_C Cluster	0.3985	7
		LCH_C Entropy	0.3904	8
		S_hsv Homogeneity	0.3691	9
		Hue Entropy	0.3664	10
Gainratio	Ranker	CMY_Y Mean	0.3846	1
		CMYK_M Energy	0.2407	2
		CMYK_M Max.Prob.	0.2623	3
		CMYK_M Contrast	0.2451	4
		CMYK_M Correlation	0.2339	5
		S_hsl Inverse	0.2328	6
		Hue Contrast	0.2254	7
		CMYK_M Entropy	0.2235	8
		S_hsv Inverse	0.2188	9
		Hue Energy	0.2109	10

Table 1 shows that the CMY-Y mean is the feature with the highest weight at 88.33. After obtaining the weights and ratings, the next step is to model the result using ANN to determine the features for predicting the level of contamination with the lowest MSE validation parameter. ANN structure with 10 selected features for estimating aflatoxin contamination in cocoa beans in fluorescence images is shown in Figure 6. ANN performance recapitulation based on several attribute evaluators showed in Table 2 and

Table 2. ANN performance recapitulation based on several attribute evaluators

No.	Attribute assessor	Search	Input feature (rank)	MSE Training	MSE Validation	R Training	R Validation
1	OneRattribute	Ranker	1~2	0.0094	0.0105	0.9919	0.9902
			1~3	0.0091	0.0088	0.9915	0.0915
			1~4	0.0092	0.0553	0.9920	0.9478
			1~5	0.0095	0.0195	0.9919	0.9806
			1~6	0.0092	0.0121	0.9921	0.9874
			1~7	0.0088	0.0238	0.9924	0.9754
			1~8	0.0078	0,1029	0.9934	0.8927
			1~9	0.0064	0.0551	0.9945	0.9469
			1~10	0.0093	0.0806	0.9926	0.9199
2	ReliefF	Ranker	1~2	0.0099	0.0191	0.9914	0.9912
			1~3	0.0100	0.0838	0.9914	0.9247
			1~4	0.0099	0.1358	0.9914	0.8905
			1~5	0.0100	0.1091	0.9913	0.9008
			1~6	0.0092	0.1327	0.9928	0.8954
			1~7	0.0098	0,1393	0.9917	0.8785
			1~8	0.0092	0.1203	0.9923	0.8867
			1~9	0.0087	0.1772	0.9927	0.8749
			1~10	0.0097	0.1401	0.9921	0.8892
3	Gainratio	Ranker	1~2	0.0095	0.0560	0.9917	0.9874
			1~3	0.0095	0.0134	0.9917	0.9907
			1~4	0.0099	0.0713	0.9916	0.9237
			1~5	0.0092	0.0535	0.9920	0.9474
			1~6	0.0094	0.1077	0.9921	0.8862
			1~7	0.0078	0.0276	0.9934	0.9706
			1~8	0.0089	0.0347	0.9923	0.9754
			1~9	0.0089	0.0438	0.9925	0.9549
			1~10	0.0094	0.0155	0.9924	0.9867

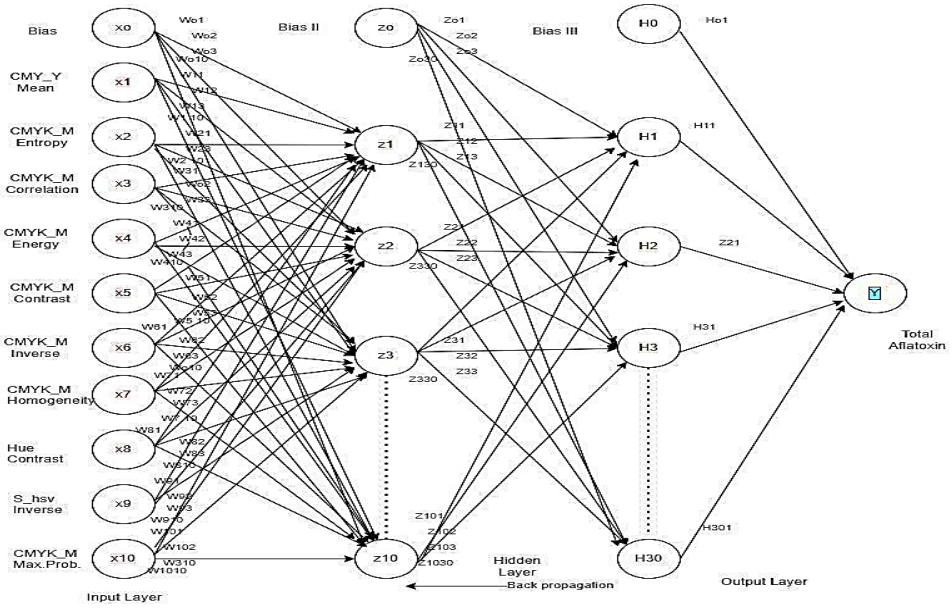

Figure 6. ANN structure with 10 input features was selected for estimating aflatoxin contamination in cocoa beans on fluorescence imagery

MSE and R value based on learning function presented in Table 3.

Based on Table 2, the best feature combination is ranked 1-3 by the OneRattribute search method. The structure of the

selected combination is then used as a basis for trial and error on the training function to determine the smallest MSE. Table 3 shows that trainlm is the selected training function that produces the smallest validation MSE. After obtaining the training function, trial and error were carried out in accordance with the activation function provided in Table 4.

Based on Table 4, the smallest MSE and the largest R-value are obtained using the tansig activation function (Hyperbolic tangent sigmoid function) with 2 hidden and 1 output layer. Subsequently, the construction of ANN architecture involves adjusting different aspects, such as learning rates, the number of nodes within hidden layers, and the number of hidden layers. These modifications are aimed at expediting the convergence of the training process and influencing the weights and biases variation during training. MSE and correlation based on variations in ANN structure is presented in Table 5.

Based on the information presented in Table 5, ANN architecture with a configuration of 3-20-20-1, A momentum value of 0.5 and a learning rate of 0.1 result in a validation MSE of 0.0087. Therefore, calculating the right number of nodes and hidden layers is an important part of creating a successful ANN structure. The sensitivity analysis is needed since more hidden layers can hinder the computation process of ANN.. Training ANN reaches the optimal condition at the maximum epoch of 5000, performance of 0.01, and maximum gradient of $1x10^{-7}$. Meanwhile, the training of the best structure is achieved at epoch 7, performance 0.00783, and

Table 3. MSE and R value based on learning function.

	Training Function	MSE Training	MSE Validation	R Training	R Validation
1	Traincgb	0.0100	0.0570	0.9919	0.9432
2	Traincgf	0.0100	0.0090	0.9914	0.9939
3	Traincgp	0.1120	0.2043	0.9075	0.8718
4	Traingd	0.0107	0.0088	0.9911	0.9935
5	Traingda	0.0106	0.0236	0.9915	0.9847
6	Traingdm	0.0106	0.0111	0.9913	0.9905
7	Traingdx	0.0100	0.0157	0.9914	0.9836
8	Trainlm	0.0091	0.0088	0.9915	0.9915
9	Trainoss	0.0100	0.0107	0.9918	0.9913
10	Trainrp	0.0099	0.0096	0.9917	0.9926

Table 4. MSE and R value based on the activation function.

Training function	Activation Function		Output layer	MSE Training	MSE Validation	R Training	R Validation
	Hidden layer 1	*Hidden layer 2*					
Trainlm	Tansig	Tansig	Tansig	0.0091	0.0088	0.9915	0.9915
	Tansig	Tansig	Purelin	0.0089	0.0587	0.9922	0.9387
	Tansig	Tansig	Logsig	0.6227	0.6173	0.9543	0.9736
	Logsig	Logsig	Purelin	0.0098	0.0268	0.9915	0.9832
	Logsig	Logsig	Tansig	0.0099	0.0093	0.9915	0.9926
	Logsig	Logsig	Logsig	0.6227	0.6237	0.9543	0.7698

Table 5. MSE and correlation based on variations in ANN structure.

Learning rate	Momentum	ANN Structure	MSE Training	MSE Validation	R Training	R Validation
0.1	0.5	3-10-1	0.0099	0.0111	0.9919	0.9905
		3-20-1	0.0100	0.0200	0.9914	0.9816
		3-30-1	0.0098	0.0132	0.9915	0.9921
		3-10-10-1	0.0099	0.0106	0.9919	0.9900
		3-20-20-1	0.0078	0.0087	0.9932	0.9910
		3-30-30-1	0.0095	0.0192	0.9918	0.9814
0.1	0.9	3-10-1	0.0100	0.0132	0.9914	0.9915
		3-20-1	0.0095	0.0132	0.9908	0.9867
		3-30-1	0.0099	0.0668	0.9918	0.9326
		3-10-10-1	0.0093	0.0098	0.9920	0.9923
		3-20-20-1	0.0091	0.0088	0.9915	0.9915
		3-30-30-1	0.0090	0.0098	0.9924	0.9912

gradient 0.00297. The relationship of total iteration and MSE in ANN training for identifying aflatoxins in cocoa beans presented in Figure 7.

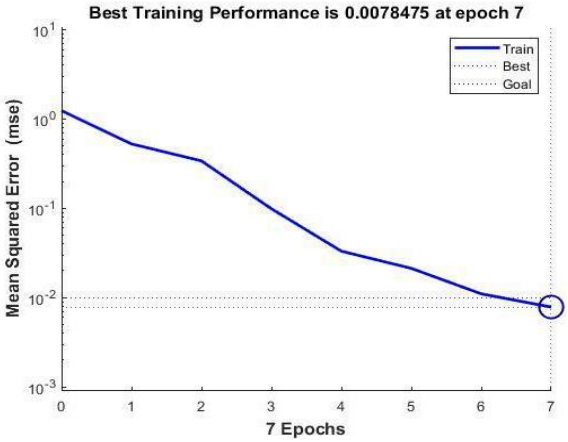

Figure 7. The relationship of total iteration and MSE in ANN training for identifying aflatoxins in cocoa beans.

In Fig. 7, the best performance is shown by the dashed blue line, and the goal is indicated by the dashed black line. Furthermore, the blue line indicates the best MSE (0.00783) with the network converging at iteration 7. The validation MSE reaches the goal of 0.01, indicating that the network accurately predicts the goal function. Another indicator that describes the performance of ANN is the R correlation value of training and validation, and the regression plot is shown in Figure 8 which shows the simulation results of the training data and validation data, marked by the blue and red lines. The training R-value obtained is 0.9932. The recapitulation of the characteristics of the input and output of the best-designed ANN is shown Table 6.

Table 6. The best ANN input and output characteristics predict the level of aflatoxin contamination.

No.	Input/output	Total/type
	Input	
1	features used as the input layer	3 (CMY_Y Mean, CMYK_M Entropy and CMYK_M correlation)
2	Total Hidden layers	3
3	Total hidden layer nodes	20
4	Total output layers	1
5	Activation function	Tansig, tansig, tansig
6	learning function	Trainlm
7	Learning rate	0.1
8	momentum	0.5
9	target error	0.01
10	Defined iteration limit (epoch)	5000
	output	
1	R Validation	0.991
2	MSE Validation	0.0087

(a)

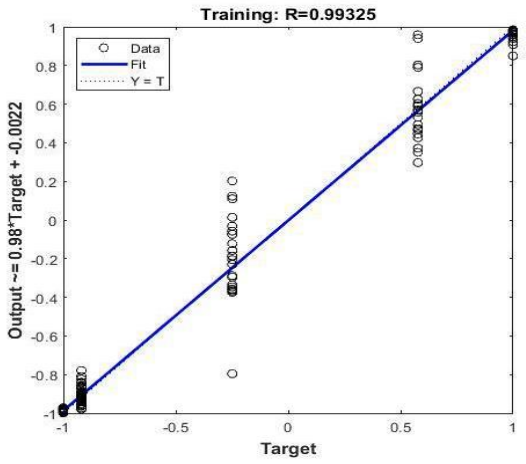

(b)

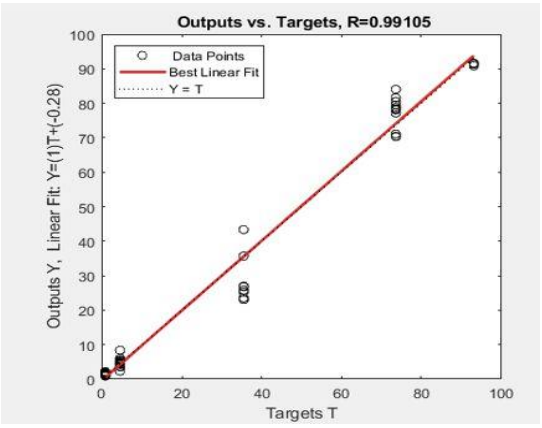

Figure 8. Regression plot of simulation results: (a) training data (b) validation data.

DISCUSSION

The results showed that on the third day of incubation, the cocoa beans had surpassed the 20 ppb threshold for total aflatoxin content. The aflatoxin levels that exceeded the limit were reported by Hruska *et al*. (2017) in maize kernels inoculated with *A. flavus*. Subsequently, the lower concentration of AFB_1 compared to AFG_1 was consistent with Pires *et al*. (2019), which examined the natural occurrence of aflatoxins in cocoa bans in Brazil.

The CMY_Y Mean, CMYK_M Entropy, CMYK_M Correlation features are selected features that will be used as input to the ANN model based on several attribute evaluators at the feature selection stage. Feature selection is a crucial step in utilizing machine learning for image prediction, as not all extracted features may be effective in predicting the objective function. Therefore, selecting the appropriate features is essential to achieve accurate and reliable predictions. According to Miao and Niu (2016), feature selection is performed on ANN to improve accuracy and reduce

computational costs. An ANN model is considered good when built based on relevant features with the output of the system, thereby improving computational performance(Khoder and Dornaika, 2021).

The trainlm training function is the selected training function in the designed ANN model. The trainlm training function is Levenberg-Marquardt algorithm training function that changes weights and bias values. The output values obtained are consistent with the findings of Sharma and K. Venugopalan, (2014), where trainlm achieved the goal performance with fewer epochs and a smaller MSE than other functions. The activation function accommodates nonlinearity in the neural network to learn complex relationships between input and output data (Abdolrasol *et al*., 2021). The selected activation function is the hyperbolic tangent because it represents a monotonic mapping between continuous variables and enables quick convergence during network training, it is frequently employed in ANN (Christiansen *et al*., 2014). The selection of the activation function may influence the validation MSE, resulting in an elevation of its value when the activation function used in training is inappropriate.

The determination of the number of goals and iterations must be achieved to minimize the occurrence of model overfitting. This is because setting the MSE goal too small can cause overfitting. Furthermore, overfitting occurs when the model tends to memorize all data, including noise in the training set, resulting in a high validation MSE (Ying, 2019). The results reveal that two hidden layers outperform one hidden layer in predicting the output variable which produce a better MSE This is due to the ability of two hidden layers to tackle non-linear problems being superior to one. This is in line with the statement of Thomas *et al*. (2017) that state 2 hidden layers are better than 1 because they can handle non-linear problems. Figure 8 showed that the prediction value for the level of aflatoxin contamination are close to the actual value because the distribution is close to the linear fit line. A low level of validation The R-value indicates that the data point distribution deviates from the linear fit on the regression plot. The R-value demonstrates the correlation between the input and output variables, and when it approaches one, it implies a strong relationship. Therefore, the R-value approaches 1, meaning the CMY_Y Mean, CMYK_M Entropy, and CMYK_M Correlation feature data have a strong relationship with the level of aflatoxin contamination in cocoa beans. Table 6 shows the overall input and output recapitulation of the ANN architecture that has been designed. The results show that the ANN model exhibits a high prediction performance. These results are in accordance with the statement by Khaliduzzaman *et al*. (2023) that fluorescence imaging is a quick and easy method with high predictive accuracy compared to traditional aflatoxin testing methods. The findings in this research, namely computer vision based on ANN and UV fluorescence is a novel method which can be applied to industry, especially the inspection of cocoa beans contaminated with aflatoxin. The advantages of this approach are reducing potential legal problems due to aflatoxin contamination, reducing defective products and consumer complaints.

***Conclusion*:** The results conclude that three color-texture features, namely CMY_Y Mean, CMYK_M Entropy, and CMYK_M Correlation, are input into ANN based on feature selection using the filter method with the OneRattribute evaluator. The best ANN structure for predicting the level of aflatoxin contamination is 3-20-20-1, with a learning rate of 0.1 and a momentum value of 0.5. Furthermore, the activation function is tansig on two hidden and output layers, and the learning function is trainlm, which will produce a validation MSE and R-value of 0.0087 and 0.9910. This indicates that UV-induced fluorescence imaging and ANN can be an alternative for predicting the level of aflatoxin contamination in cocoa beans.

***Authors contributions statement*:** MSS conducting research and writing manuscript. BDA conducting research and review manuscript. SS conducting research and review manuscript. DFA conducting research and provide hardware. YH conducting research and review manuscript.

***Conflict of interest*:** The authors declare no conflict of interest.

Acknowledgment: The authors would like to acknowledge KEMENDIKBUD-RISTEK, Lembaga Pengelola Dana Pendidikan (LPDP), and Beasiswa Pendidikan Indonesia (BPI) Indonesia for scholarship funding.

***Funding statement*:** This research funded by KEMENDIKBUD-RISTEK, Lembaga Pengelola Dana Pendidikan (LPDP), and Beasiswa Pendidikan Indonesia (BPI) Indonesia.

***Ethical statement*:** This article does not contain any studies regarding human or Animal.

***Availability of data and material*:** We declare that the submitted manuscript is our work, which has not been published before and is not currently being considered for publication elsewhere.

***Code availability*:** Not applicable.

***Consent to participate*:** All authors participated in this research study.

***Consent for publication*:** All authors submitted consent to publish this research. article in JGIAS.

REFERENCES

Abdolrasol, M.G.M., S.M. Hussain, T.S. Ustun, M.R. Sarker, M.A. Hannan, R. Mohamed, J.A. Ali, S. Mekhilef and A. Milad. 2021. Artificial neural networks based optimization techniques: A review. Electronics 10:55-64

Adriansyah, P.N.A., W.P. Rahayu, H.D. Kusumaningrum and O. Kawamura. 2022. Aflatoxin M1 reduction by microorganisms isolated from kefir grains. International Food Research Journal 29:78-85.

Amin, M.A., M.K. Hanif, M.U. Sarwar, A. Rehman, F. Waheed and H. Rehman. 2019. Parallel backpropagation neural network training techniques using Graphics Processing Unit. International Journal of Advanced Computer Science and Applications 10:563-566.

Anami, B.S., N.M. Naveen and N.G. Hanamaratti. 2015. Behavior of HSI Color Co-Occurrence Features in Variety Recognition from Bulk Paddy Grain Image Samples. International Journal of Signal Processing, Image Processing and Pattern Recognition 8:19-30.

Bhensjaliya, A.H. and H.D.Vasava. 2019. Survey on Classification of Rice Grains Using Neural Network. International Journal of Computer Sciences and Engineering 7:828-831.

Cabrera-Meraz, J., L. Maldonado, A. Bianchini and R. Espinal. 2021. Incidence of aflatoxins and fumonisins in grain, masa and corn tortillas in four municipalities in the department of Lempira, Honduras. Heliyon 7:

Chen, D., C. Guo, W. Lu, C. Zhang and C. Xiao. 2023. Rapid quantification of royal jelly quality by mid-infrared spectroscopy coupled with backpropagation neural network. Food Chemistry 418:135996.

Christiansen, N.H., P.E.T. Voie, O. Winther and J. Høgsberg. 2014. Comparison of neural network error measures for simulation of slender marine structures. Journal of Applied Mathematics 2014.

Copetti, M.V, B.T. Iamanaka, J.I. Pitt and M.H. Taniwaki. 2014. Fungi and mycotoxins in cocoa: from farm to chocolate. International Journal of Food Microbiology 178:13-20.

Cozzini, P., G. Ingletto, R. Singh and C. Dall'Asta. 2008. Mycotoxin detection plays "cops and robbers": Cyclodextrin chemosensors as specialized police? International Journal of Molecular Sciences 9:2474-2494.

Da Silva, J.V.B., C.A.F. de Oliveira and L.N.Z. Ramalho. 2021. Effects of Prenatal Exposure to Aflatoxin B1: A Review. Molecules 26:35-42

Dachoupakan S.C., R. Putthang and P. Sirisomboon. (2013). Application of near infrared spectroscopy to detect aflatoxigenic fungal contamination in rice. Food Control 33:207-214.

Du, Z., N. Ali and B. Ashraf. 2019. X - ray computed tomography for quality inspection of agricultural products : A review March:3146-3160.

European Commission. 2014. Commission Implementing Regulation (EU) No 884/2014 of 13 August 2014 imposing special conditions governing the import of certain feed and food from certain third countries due to contamination risk by aflatoxins and repealing Regulation (EC) No 1152/2009. Official Journal of the European Union 2001:20-30.

Fang, L., B. Zhao, R. Zhang, P. Wu, D. Zhao, J. Chen, X. Pan, J. Wang, X. Wu, H. Zhang, X. Qi, J. Zhou and B. Zhou, 2022. Occurrence and exposure assessment of aflatoxins in Zhejiang province, China. Environmental Toxicology and Pharmacology 92:103847.

Ford, A. and A.R. Alanrobertsrdbbccouk.1998. Colour Space Conversions 1998:1-31.

Galaverna, G. and C. Dall'Asta. 2012. 4.16 - Sampling Techniques for the Determination of Mycotoxins in Food Matrices (J. B. T.-C. S. and S. P. Pawliszyn (ed.); pp. 381–403.

Gao, J., L. Zhao, J. Li, L. Deng, J. Ni and Z. Han. 2021. Aflatoxin rapid detection based on hyperspectral with 1D-convolution neural network in the pixel level. Food Chemistry 360:129968.

Haralick, M.R., K. Shanmugam and I. Distein. 1973. Textural Features for Image Classification'. IEEE.

Hassoun, A. and R. Karoui. 2015. Quality Evaluation of Fish and Other Seafood by Traditional and Nondestructive Instrumental Methods: Advantages and Limitations. Critical Reviews in Food Science and Nutrition 57: 11-16

Hendrawan, Y., S. Widyaningtyas and S. Sucipto. 2019. Computer vision for purity, phenol, and pH detection of Luwak coffee green bean. Telkomnika 17:3073-3085.

Hruska, Z., H. Yao, R. Kincaid, R.L. Brown, D. Bhatnagar and T.E. Cleveland. 2017. Temporal effects on internal fluorescence emissions associated with aflatoxin contamination from corn kernel cross-sections inoculated with toxigenic and atoxigenic Aspergillus flavus. Frontiers in Microbiology 8:1-10.

Kamilaris, A. and F.X. Prenafeta-Boldú. 2018. A review of the use of convolutional neural networks in agriculture. Journal of Agricultural Science 156:312-322.

Kaur, H. and B. Singh. 2013. Classification and Grading Rice Using Multi-Class SVM. International Journal of Scientific and Research Publications 3:1–5.

Kaya-celiker, H., P.K. Mallikarjunan and A. Kaaya. 2015. Mid-infrared spectroscopy for discrimination and classi fi cation of Aspergillus spp . contamination in peanuts. Food Control 52:103-111.

Ketney, O. 2015. Food Safety Legislation Regarding Of Aflatoxins Contamination. ACTA Universitatis Cibiniensis 67:149-154.

Khaliduzzaman, A., K.A. Omwange, D.F. Al Riza, K. Konagaya, M. Kamruzzaman, M.S. Alom, T. Gao, Y.

Saito and N. Kondo. 2023. Antioxidant assessment of agricultural produce using fluorescence techniques: a review. Critical Reviews in Food Science and Nutrition 63:3704-3715.

Khoder, A. and F. Dornaika. 2021. Ensemble learning via feature selection and multiple transformed subsets: Application to image classification. Applied Soft Computing 113:108006.

Kong, D., G. Wang, Y. Tang, M. Guo, Z. Ul Haq Khan, Y. Guo, W. Gu, Y. Ma, M. Sui, J. Li, and M. Yang. 2022. Potential health risk of areca nut consumption: Hazardous effect of toxic alkaloids and aflatoxins on human digestive system. Food Research International 162:112012.

Mallmann, C.A., A.O. Mallmann and D. Tyska. 2020. Survey of Mycotoxin in Brazilian Corn by NIR Spectroscopy-Year 2019:1-7.

Marcial-Pablo, M.de J., A. Gonzalez-Sanchez, S.I. Jimenez-Jimenez, R.E. Ontiveros-Capurata and W. Ojeda-Bustamante. 2019. Estimation of vegetation fraction using RGB and multispectral images from UAV. International Journal of Remote Sensing 40:420-438.

Miao, J. and L. Niu. 2016. A Survey on Feature Selection. Procedia Computer Science 91: 919-926.

Oliveira, C.A.F., N.B. Gonçalves, R.E. Rosim and A.M. Fernandes. 2009. Determination of aflatoxins in peanut products in the northeast region of São Paulo, Brazil. International Journal of Molecular Sciences 10:174-183.

Osaili, T.M., W.A. Odeh, M.B.Ayoubi, M. Al, A.A. Ali, S.A. Al, M.S. Al, Obaid, R.S.Garimella, V. Bakhit, F. S. Bin, R. Holley and N.El. Darra. 2023. Occurrence of aflatoxins in nuts and peanut butter imported to UAE. Heliyon 9: e14530.

Patil, N.K., V.S. Malemath and R.M. Yadahalli. 2011. Color and Texture Based Identification and Classification of food Grains using different Color Models and Haralick features. International Journal on Computer Science and Engineering 3:3669-3680.

Pires, P.N., E.A. Vargas, M.B. Gomes, C.B.M. Vieira, E.A. Santos, A.A.C. Bicalho, S.de C. Silva, R.P. Rezende, I.S. Oliveira, E.D.M.N. De Luz and A.P. Trovatti Uetanabaro. 2019. Aflatoxins and ochratoxin A: occurrence and contamination levels in cocoa beans from Brazil. Food Additives and Contaminants-Part A Chemistry, Analysis, Control, Exposure and Risk Assessment 36:815-824.

Polisenska, I. 2011. Identification of Fusarium damaged wheat kernels using image analysis. Acta Universitatis Agriculturae Et Silviculturae Mendelianae Brunensis 59:125-130.

Saravanan, G., G. Yamuna and S. Nandhini. 2016. Real Time Implementation of RGB to HSV/ HSI/ HSL and Its Reverse Color Space Models 5:462-466.

Shabeer, S., S. Asad, A. Jamal and A. Ali. 2022. Aflatoxin Contamination, Its Impact and Management Strategies: An Updated Review. Toxins 14: 51-62

Sharma, B. and K.P Venugopalan. 2014. Comparison of Neural Network Training Functions for Hematoma Classification in Brain CT Images. IOSR Journal of Computer Engineering 16:31-35.

Tallada, J. G., D.T. Wicklow, T.C. Pearson and P.R. Armstrong. 2011. Detection of Fungus-Infected Corn Kernels using Near-Infrared Reflectance Spectroscopy and Color Imaging. Transactions of the ASABE 54:1151-1158.

Thiruppathi, S. 2016. Near-Infrared (NIR) hyperspectral imaging : theory and applications to detect fungal infection and mycotoxin contamination in food products Journal of Grain Storage Research 1:90-99

Thomas, A., M. Petridis, S. Walters, S. Malekshahi Gheytassi and R. Morgan. 2017. Two Hidden Layers are Usually Better than One. Engineering Applications of Neural Networks 12:279-290

Van Der Fels-Klerx, H.J., C. Liu and P. Battilani. 2016. Modelling climate change impacts on mycotoxin contamination. World Mycotoxin Journal 9:717-726.

Venora, G., O. Grillo and R. Saccone. 2009. Quality assessment of durum wheat storage centres in Sicily: Evaluation of vitreous, starchy and shrunken kernels using an image analysis system. Journal of Cereal Science 49:429-440.

Vivek, V., S. Bermúdez and C. Larrea. 2019. Global Market Report: Cocoa. Exchange Organizational Behavior Teaching Journal 7:1-12.

Wahyuni, S., P.E. Susilowati, Tamrin, Holilah, Asranudin, W.P. Utomo, Y. Dueris and L. Samarindu. 2016. Characterization and application of polygalacturonase from trinitario (Theobroma cacao L.) pulp. Asian Journal of Chemistry 28:2261-2266.

Ying, X. 2019. An Overview of Overfitting and its Solutions. Journal of Physics: Conference Series 1168:73-83

Zhang, L., H. Zhang, W. Han, Y. Niu, J.L. Chávez and W. Ma. 2021. The mean value of gaussian distribution of excess green index: A new crop water stress indicator. Agricultural Water Management 251.